



## Evolution of local friction along a model pile shaft in a calibration chamber for a large number of loading cycles

Hadj Bekki<sup>a</sup>, Jean Canou<sup>b,\*</sup>, Brahim Tali<sup>b</sup>, Jean-Claude Dupla<sup>b</sup>, Ali Bouafia<sup>a</sup>

<sup>a</sup> Université Saâd-Dahleb de Blida, département de génie civil, BP 270, Blida, Algeria

<sup>b</sup> Université Paris-Est, Ecole des Ponts ParisTech, laboratoire Navier - Géotechnique, 6 et 8, avenue Blaise Pascal, Champs-sur-Marne, 77455 Marne-la-Vallée, France

### ARTICLE INFO

#### Article history:

Received 22 February 2012

Accepted 22 November 2012

Available online 7 March 2013

#### Keywords:

Granular media

Pile

Friction

Calibration chamber

Sand

Cyclic loading

Cyclic softening

Cyclic hardening

#### Mots-clés :

Milieux granulaires

Pieu

Frottement

Chambre d'étalonnage

Sable

Chargement cyclique

Ramollissement cyclique

Durcissement cyclique

### ABSTRACT

This Note presents the results of axial loading tests carried out on an instrumented “pile-probe” jacked into sand, in a calibration chamber, aimed at studying the evolution of local friction, up to very large numbers of cycles ( $10^5$  cycles). After an initial phase of friction degradation (cyclic softening), a subsequent phase of mobilized friction reinforcement (cyclic hardening) is observed, which continues to develop up to very large numbers of cycles. The complete mechanism of shear degradation followed by the reinforcement phase is interpreted based on the competition between two mechanisms which are the mean normal effective stress decrease due to cyclic contractancy phenomenon, responsible for cyclic softening, and the progressive densification of the sand within the interface zone around the probe, which becomes predominant after a certain number of cycles, resulting in a cyclic hardening mechanism due to partially constrained dilatancy phenomenon.

© 2012 Académie des sciences. Published by Elsevier Masson SAS. All rights reserved.

### R É S U M É

On présente dans cette Note les résultats d'essais de chargement axial d'une sonde-pieu instrumentée dans des massifs de sable reconstitués en chambre d'étalonnage, destinés à étudier l'évolution du frottement latéral local dans des chargements cycliques, menés à grands nombres de cycles ( $10^5$  cycles). Après une phase initiale de dégradation du frottement latéral (radoucissement cyclique), on met en évidence une phase de ré-augmentation du frottement (durcissement cyclique), qui se poursuit jusqu'aux grands nombres de cycles. Le mécanisme global de dégradation suivi du renforcement est interprété en mettant en avant la compétition entre deux mécanismes concurrents, qui sont la diminution de contrainte normale effective moyenne due au phénomène de contractance cyclique (responsable de la dégradation) et le phénomène de dilatance empêchée, qui s'accroît avec la densification progressive du sable dans la zone d'interface autour de la sonde.

© 2012 Académie des sciences. Published by Elsevier Masson SAS. All rights reserved.

## 1. Introduction

The understanding of the behaviour of deep foundations under cyclic loading constitutes an important issue in the domain of geotechnical engineering, related to the design of the foundations of various civil engineering structures, submitted to environmental and/or industrial types of “cyclic” loading. For axial loads, in particular, the load applied at the pile head

\* Corresponding author.

E-mail address: [jean.canou@enpc.fr](mailto:jean.canou@enpc.fr) (J. Canou).

is taken by both friction, mobilized along the pile shaft, and tip resistance mobilized at the pile tip. In the domain of cyclic axial loadings, which are usually superimposed to the static loads resulting mainly from the structure weight, the question arises of the evolution of the shaft friction properties due to the application of the loading cycles.

Since the beginning of the 1980s, quite a few research studies have been carried out in this field, mainly in relation with the offshore oil production industry and the design of foundations for offshore oil production platforms [1–7]. As far as experimental research is concerned, three main types of experimental approaches have been developed: interface tests in modified shear boxes (linear, annular) allowing one to track “elementary” behaviour of the interface [8–10]; physical modelling approaches in which instrumented probes, representing piles or pile elements at reduced scale, are installed and loaded in reconstituted large size samples of soil representative of the soil around the pile, in 1 g models like calibration chambers experiments and macrogravity models in centrifuges [11–14]; full size or semi full size experiments performed on specific experimental sites or during civil engineering construction works [3,15,16].

These studies have generally been concerned with a small to medium number of cycles, namely a few tens to a few thousands, representing, for example, storm loadings. Most studies have reached conclusions confirming a degradation process for local friction due to cyclic loading.

Based on a series of two-way displacement-controlled interface tests on dry crashed silica sand using a modified direct shear box, carried out for both constant normal stress and constant normal stiffness conditions (50 to 55 cycles, frequency  $f = 0.005$  Hz), Fakharian and Evgin [9] have noted a significant reduction of maximum shear stress mobilized with cycles, in particular during the first cycles.

Lee and Poulos [17] have conducted cyclic displacement-controlled and force-controlled tests (100 to 500 cycles) on model piles (24 mm diameter) installed into medium dense calcareous sediments, in order to study the degradation of skin friction for grouted piles. Their results showed that the degradation of skin friction depends on the amplitude of cyclic displacement and number of cycles.

Chin and Poulos [7] have conducted cyclic displacement-controlled tests (100 to 150 cycles) on model piles (5 cm and 10 cm in diameter) installed in a calcareous sand reconstituted in a calibration chamber (1 m diameter). These authors found that the degradation of skin friction is governed by a “cyclic slip displacement” parameter and they also noted the presence of a limit degradation factor corresponding to a maximum degradation of the pile–soil interface.

Le Kouby et al. [12] have studied the degradation of local skin friction in a calibration chamber for two-way cyclic displacement-controlled loading tests (50 cycles) carried out on an instrumented 20 mm diameter probe. The results showed a very significant degradation of skin friction due to cycling loading.

Foray et al. [14] measured both normal and shear stresses acting locally on the shaft of an instrumented model pile during cyclic loading in a calibration chamber. The authors performed 100 to 1000 one-way load-controlled cycles in traction and about 100 two-way load-controlled cycles. Plotting the corresponding “stress path” in the stress plane, they observed a succession of contraction and dilation phases with a progressive reduction of the normal stress explaining the degradation of skin friction.

As far as a large to a very large number of cycles is concerned ( $10^4$  to  $10^6$  cycles), which may be found in industrial types of loading (traffic, rotating/vibrating machines, wind turbines, etc.) characterized by fatigue behaviour of the soil–structure interface, very few results, if no results at all, have been published.

Within this general framework, a national research programme, called SOLCYP, involving different research laboratories and industrial organisms, has been undertaken in France in 2008 with the aim of better understanding the behaviour of piles submitted to large numbers of cycles, in order to improve their design. Within this programme, a specific research action has been undertaken in our laboratory with the aim of studying the evolution of local pile shaft friction for very large numbers of cycles (up to  $10^5$  cycles), using a physical modelling approach based on the use of a calibration chamber experimental set-up.

The objective of this Note is to present the results of typical tests carried out within this research programme, representative of most tests carried out and to focus on the predominant feature observed for large numbers of cycles, i.e. a cyclic hardening phenomenon of local friction.

After presentation of the experimental set-up and testing procedure, the results of a representative test are presented, allowing to observe, after an initial expectable degradation phase of local friction (cyclic strain-softening), a reinforcement phase (cyclic strain-hardening) which keeps developing until the end of the cyclic sequence reached at a very high number of cycles.

## 2. Experimental set-up and testing procedure

### 2.1. Experimental set-up

The calibration chamber set-up is an experimental facility which allows to reconstitute and put under stress large size samples of soil (sand in this case) under well-controlled conditions (state of stress, sand density, homogeneity), simulating a “slice” of soil located at a given depth. It is then possible to simulate, within the reconstituted soil sample, a given process or phenomenon, thus developing a physical modelling approach of a given geotechnical problem. A functional scheme of the experimental set-up is presented in Fig. 1. The sample of sand has a diameter of 52 cm and a height of 70 cm. It is reconstituted using pluviation technique, which allows one to obtain a very good homogeneity of the sand within the

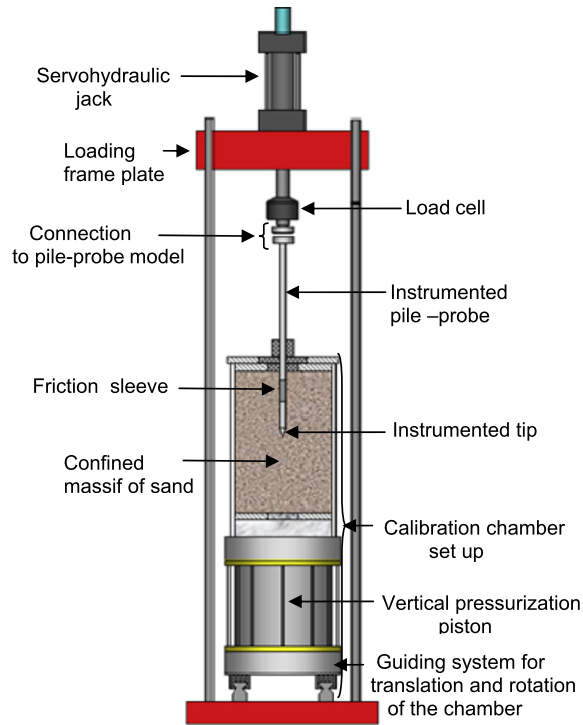
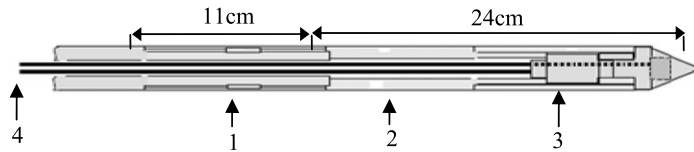


Fig. 1. Functional scheme of the experimental set-up.



- 1 : Instrumented friction sleeve
- 2 : Body of the probe
- 3 : Force transducer for tip resistance measurement
- 4 : Transducers cables

Fig. 2. Schematic cross-section of the pile-probe (Ø 36 mm, [19]).

massif, at a given state of density (characterized by the density index  $I_D$ ), depending on the mass flow rate and pluviation height used during the pluviation process [18]. After pluviation, the sand is put under stress by applying two independent water pressures, one, applied inside the lateral confinement wall, allowing to horizontally confine the sand contained in a rubber membrane, the other one, applied in the base piston of the chamber, allowing to vertically pressurize the sand. This procedure allows one to follow different stress paths to reach an initial state of effective stress (isotropic or anisotropic), characterized by  $\sigma'_{v0}$  (vertical stress) and  $\sigma'_{h0}$  (horizontal stress).

In order to simulate the installation and the loading of a pile element, a specific prototype instrumented “pile-probe” has been developed [19]. Fig. 2 presents a functional scheme of the probe, which allows to measure independently tip resistance  $q_p$  mobilized at the conical tip of the probe and local friction  $f_s$  mobilized on a friction sleeve located far enough from the probe tip. The probe has a cross-section of  $10 \text{ cm}^2$  (diameter 3.6 cm). The friction sleeve is 11 cm long (section of  $124.4 \text{ cm}^2$ ), which allows one to use the hypothesis of stress uniformity along the sleeve to convert shear forces to shear stresses. The sleeve is made up of a special hard steel, which has been specifically machine-shopped to provide a controlled roughness corresponding to a “perfectly rough” interface, with respect to the mean size of the sand used (depth of groove, crest to crest, equal to  $35 \mu\text{m}$ ).

## 2.2. Testing procedure

After reconstitution and pressurization of the sample of sand, the “pile-probe” is first pushed into the sand at constant displacement rate (1 mm/s) with a long stroke classical hydraulic jack, which simulates a full-displacement installation process for a pile. After installation, the configuration is such that the friction sleeve is approximately centred within the

**Table 1**  
Main characteristics of Fontainebleau sand NE34.

$e_{\min}$	$e_{\max}$	$D_{50}$ (mm)	$\rho_s$ (t/m <sup>3</sup> )
0.510	0.882	0.205	2.65

sample, far away from the top and bottom end plates, thus minimizing boundaries influence. The probe can subsequently be loaded with a servo-controlled hydraulic jack, through a digital control unit which allows to run displacement-controlled or force-controlled monotonic and cyclic tests according to a predefined loading program. A very high number of cycles may be reached (up to several  $10^5$  cycles), in the range of fatigue behaviour. Frequencies up to 50 to 60 Hz may also be reached, depending on the problem to be studied and the displacement amplitudes required.

Usually, a monotonic displacement-controlled (300  $\mu\text{m}/\text{min}$ ) push-in loading is first applied, after installation, in order to obtain failure characteristics in terms of tip resistance and ultimate shaft friction. The cyclic displacement-controlled sequence is then performed, followed by a final monotonic loading which allows one to obtain final failure characteristics that may be compared to initial characteristics.

### 3. Presentation of a typical test

The aim of the research undertaken within the SOLCYP project was to investigate, based on the experimental facility described above, the evolution of local friction along a pile shaft model submitted to large numbers of cycles ( $10^5$  cycles). In particular, a complete experimental programme, corresponding to the reconstitution of more than 30 samples, has been carried out over a three years period of time, in order to study the influence of such parameters as initial state of sand (density index and state of consolidation stress), amplitude and frequency of cyclic loading, diameter of probe and installation process, on the results obtained. This work has been the object of the Ph.D. thesis of Tali [20] and Bekki, the latter being under development.

The objective of this Note is not to present a comprehensive analysis of the whole experimental programme carried out, which would be beyond its scope, but to focus on a specific predominant phenomenon observed, which has been consistently retrieved all along the study, with slight modulations in function of testing parameters values. This phenomenon is the cyclic hardening of the interface behaviour, which develops for large numbers of cycles, after an initial phase of cyclic softening.

It is important to mention here that consistent results were obtained over the whole testing period, accounting for no significant evolution of testing parameters such, for example, as sleeve roughness. Also, the room temperature was fairly well controlled during the tests, with fluctuations less than 2 °C on a daily period (night and day), which would not influence significantly test results.

#### 3.1. Description of the test

The test selected and presented below (Test 1) has been carried out in a sample of dry Fontainebleau sand (reference NE34), prepared in a dense initial state ( $I_D = 0.90$ ). The main characteristics of this sand are presented in Table 1. The state of stress applied to the massif corresponds to a vertical stress  $\sigma'_{v0}$  equal to 125 kPa and a horizontal stress  $\sigma'_{h0}$  equal to 50 kPa. After installation of the probe and initial monotonic loading to failure, the probe has been subjected to a cyclic displacement-controlled loading test up to 100 000 cycles, applied at a frequency of 1 Hz, for a displacement amplitude  $\rho_c$  equal to  $\pm 500$   $\mu\text{m}$  (alternated signal). Fig. 3(a) presents the sinusoidal displacement  $\rho$  applied as a function of number of cycles  $N$  (logarithmic scale for  $N$ ). This type of displacement-controlled test (analogous to cyclic strain-controlled tests in a triaxial test for example) allows to study the evolution of friction mobilization with number of cycles (cyclic strain-softening or strain-hardening). Fig. 3(b) presents the response observed in terms of the friction mobilized versus number of cycles. This type of representation allows one to immediately visualize the maxima and minima of friction reached for each cycle and define an envelope curve showing degradation zones and reinforcement zones. It may be seen from this figure that, after an initial phase of friction degradation, up to about 300 cycles, a phase of progressive hardening of the interface behaviour is observed, which regularly continues up to the end of the cyclic sequence, reached after  $10^5$  cycles.

The strain-softening (or degradation) part of the curve is in good agreement with observations previously made by different authors (see above). However, the strain-hardening (or reinforcement) part, which occurs subsequently, has not, to our knowledge, been described before. This result shows that friction degradation would not keep going continuously for large numbers of cycles but, after reaching a minimum of mobilized friction [7], a reinforcement phase would be observed and would keep developing up to very large numbers of cycles.

Fig. 4 presents a few selected cycles plotted in the  $(f_s, \rho)$  plane. Fig. 4(a) allows one to observe the cyclic degradation or cyclic strain-softening of the interface behaviour, which starts practically at cycle n° 1 and keeps going up to cycle n° 300. It is interesting to note the strong non-linearity of the cycles' shape, which accounts for a cyclic displacement amplitude which is fairly large with respect to the probe diameter, and a strongly non-reversible behaviour of the interface. The non-linearity of the cycles increases regularly with the number of cycles, with a regular decrease of maxima reached upon "push-in" phases,  $f_{s,\max}$ , and absolute values of minima,  $f_{s,\min}$ , reached upon "pull-out" phases.

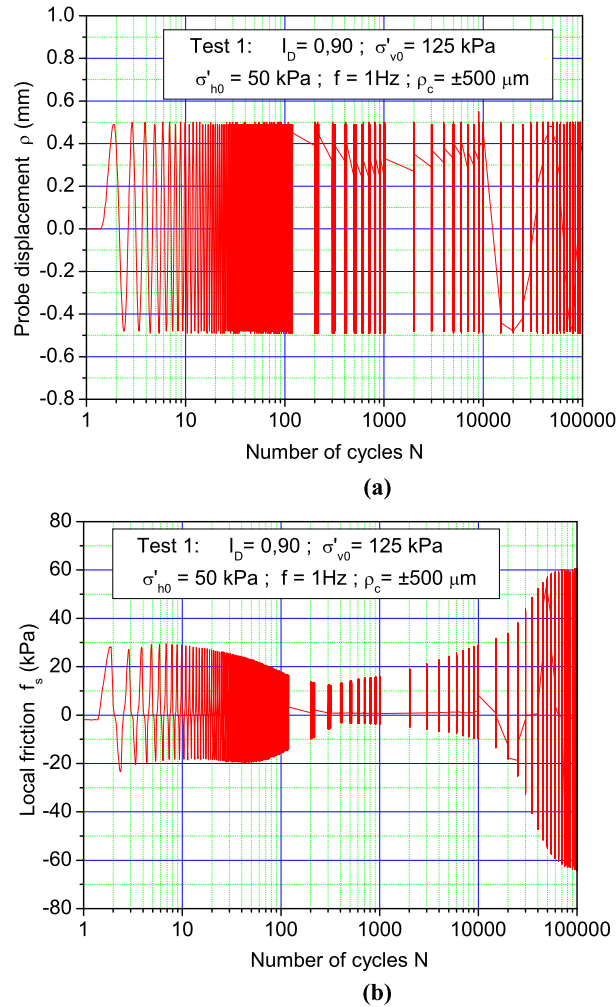


Fig. 3. Results of typical test (Test 1): (a) displacement-controlled loading signal; (b) response obtained in terms of local friction versus number of cycles.

Fig. 4(b) shows, on the contrary, a clear phenomenon of cyclic strain-hardening (or cyclic reinforcement) which develops regularly after the initial degradation phase, from cycle n° 300 to cycle n° 100 000 (end of the test), for which significantly higher values of  $f_{s,max}$  and  $f_{s,min}$  ( $\pm 60$  kPa) are obtained, with respect to the first cycle (30 and  $-24$  kPa) and, a fortiori, with respect to cycle n° 300. It is also interesting to note that the cycles become almost symmetrical with respect to the axes for large numbers of cycles, and highly non-linear.

### 3.2. Coefficient of friction evolution

In order to represent in a synthetic way the evolution of lateral friction mobilized during cyclic loading, a coefficient of friction evolution has been defined as follows:

$$C_{e,f_s} = \frac{f_{s,max(i)} - f_{s,min(i)}}{f_{s,max(1)} - f_{s,min(1)}}$$

where:  $f_{s,max(1)}$  and  $f_{s,max(i)}$  are the maximum values of skin friction measured on the first cycle and on cycle  $i$ , respectively (push-in phases);  $f_{s,min(1)}$  and  $f_{s,min(i)}$  are the minimum values of skin friction measured on the first cycle and on cycle  $i$  respectively (pull-out phases).

This coefficient takes into account the maximum value of friction reached upon “push-in” phases and the minimum value reached upon “pull-out” phases, which allows to define a parameter representative of the average evolution (degradation or reinforcement) of the complete cycle, with respect to the first cycle applied. Fig. 5 shows such a representation of the test described above in terms of  $C_{e,f_s}$  versus number of cycles. This type of representation allows one to rapidly identify degradation and reinforcement phases versus number of cycles. For the specific test presented, maximum degradation occurred at cycle n° 300 with a value of  $C_{e,f_s}$  equal to 0.42 and maximum reinforcement was observed for the last cycle, n° 100 000.

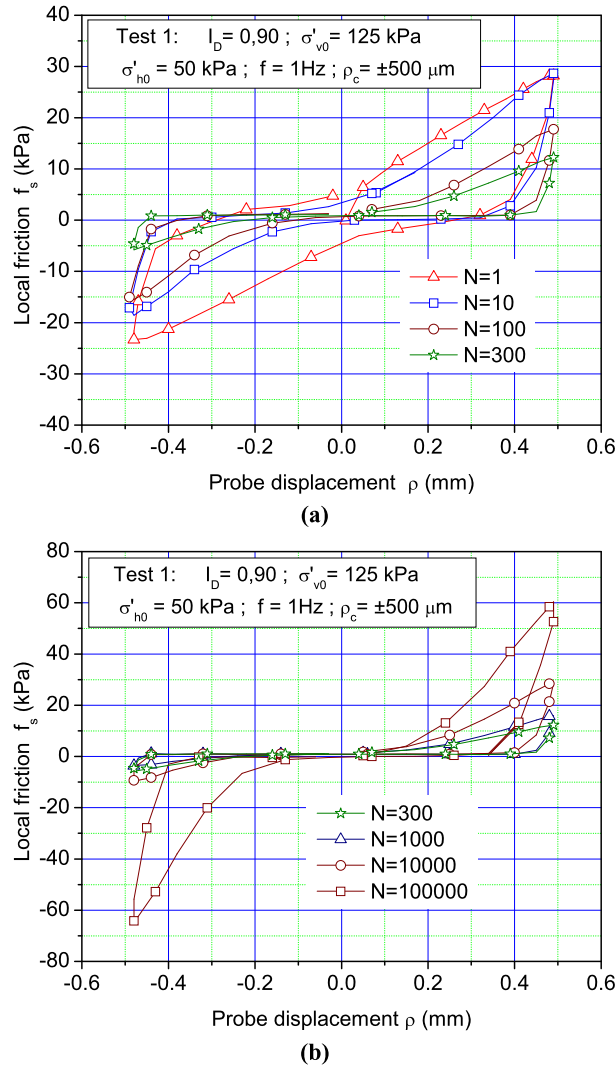


Fig. 4. Representation of selected friction cycles for Test 1: (a) cyclic softening phase (cycles 1 to 300); (b) cyclic hardening phase (cycles 300 to 100000).

Table 2  
Main tests characteristics.

Test identification	Density index $I_D$	$\sigma'_{v0}$ (kPa)	$\sigma'_{h0}$ (kPa)	Frequency $f$ (Hz)	$\rho_c$ ( $\mu$ m)	Number of cycles	Observations
Test 1	0.90	125	50	1	$\pm 500$	100 000	
Test 2	0.90	125	50	1	$\pm 500$	100 000	Repeatability test

It is interesting to note the high value of  $C_{e, f_s}$  at the end of the cyclic sequence, equal to about 2.2, which accounts for a significant strain-hardening due to the cycles in this test.

### 3.3. Test of repeatability

In order to confirm the results presented above, a repeatability test (Test 2, Table 2) has been carried out for same testing conditions and parameters as Test 1. Fig. 5 also shows a comparison of the results obtained for both tests in terms of  $C_{e, f_s}$  versus number of cycles, which confirms a good repeatability of the test and the “meaningful” nature of the results obtained in terms of local friction evolution versus number of cycles.

### 3.4. Confirmation of observations made for different testing conditions

As already mentioned in previous sections of the paper, a similar cyclic hardening phenomenon has been observed in most tests carried out within this research programme, corresponding to various testing conditions (parametric study performed).

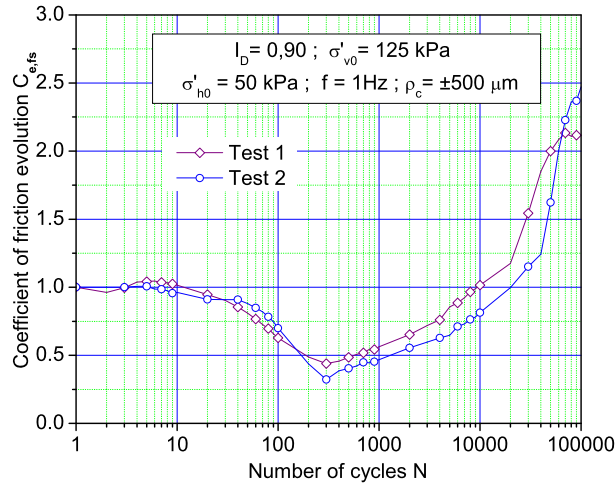


Fig. 5. Coefficient of friction evolution  $C_{e,fs}$  versus number of cycles, for Test 1 and Test 2 (evaluation of repeatability).

Table 3

Maximum values of  $C_{e,fs}^{max}$  obtained for various testing conditions.

Test identification	Density index $I_D$	$\sigma'_{v0}$ (kPa)	$\sigma'_{h0}$ (kPa)	Frequency $f$ (Hz)	$\rho_c$ ( $\mu\text{m}$ )	Number of cycles	$C_{e,fs}^{max}$
Test 1	0.90	125	50	1	$\pm 500$	$10^5$	2.14
Test 2	0.90	125	50	1	$\pm 500$	$10^5$	2.48
Test 3	0.65	125	50	1	$\pm 250$	$10^5$	1.61
Test 4	0.65	125	50	1	$\pm 500$	$10^5$	3.34
Test 5	0.65	250	100	1	$\pm 500$	$10^5$	1.53
Test 6	0.65	250	100	1	$\pm 250$	$10^5$	2.70
Test 7	0.40	125	50	1	$\pm 250$	$10^5$	1.18
Test 8	0.40	125	50	1	$\pm 500$	$10^5$	4.75
Test 9	0.40	250	100	1	$\pm 250$	$10^5$	1.59
Test 10	0.40	250	100	1	$\pm 500$	$10^5$	2.98

In order to illustrate this, Table 3 presents the results obtained for ten representative tests selected within the experimental programme, in terms of the maximum value,  $C_{e,fs}^{max}$ , for a given test, of the coefficient of friction evolution defined in Section 3.2. Values of this parameter higher than 1 account for a cyclic hardening phenomenon occurring during the cyclic sequence. Table 3 clearly shows that, for various initial and loading conditions, i.e. initial state of sample in terms of density index (very dense, medium dense and loose states) and initial state of stress of sample (two different stress states tested), and different amplitudes of cyclic loading ( $\pm 250 \mu\text{m}$  and  $\pm 500 \mu\text{m}$ ), values of  $C_{e,fs}^{max}$  significantly higher than 1 are obtained, which confirms the observations done for the two typical tests presented and analyzed before (Test 1 and Test 2 in the table) and the consistency of the phenomenon described and interpreted in this paper.

#### 4. Interpretation of results

The initial degradation phenomenon observed during the first hundreds of cycles is relatively “classical” and it has already been observed by different authors [7,9,12,14,17]. However, the phenomenon of cyclic hardening which subsequently occurs and keeps developing up to large numbers of cycles, has not, to our knowledge, been the object of previous observations. It is important to note that in most cases, published results concern small to medium numbers of cycles (few tens to few thousands) and we did not find any results concerning large to very large numbers of cycles, range in which the hardening phenomenon is observed. The interpretation of the observed behaviors can be done using a relatively simple mechanical model, based on the concept of constant rigidity of the soil surrounding an interface zone around the probe, as shown in Fig. 6, with a spring of stiffness  $k_0$  representing the rigidity of the surrounding soil. This model has already been described and used by different authors for interpreting behaviour observed under monotonic loading [13,21] and friction degradation observed under cyclic loading [22]. It appears this model could still be valid to explain the behaviour described above, and, in particular, the strain-hardening phase, as explained below.

It must be noted here that the interpretation proposed is based on a hypothesis of no significant evolution of the sand within the interface during cyclic loading. Based on the use of two installation modes for the probe (no displacement and full displacement modes) and on the analysis of grain size distribution after cyclic testing, it was shown [20] that the cyclic sequence does not modify significantly the sand (no significant grain crushing), which appears reasonable since

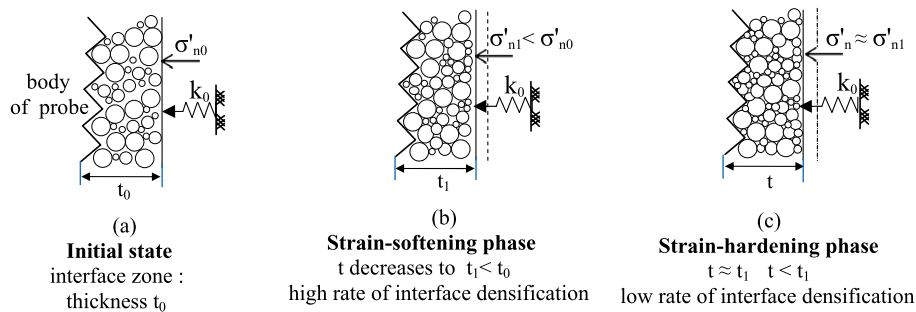


Fig. 6. Conceptual model for interpretation of friction evolution during cyclic loading.

the displacement amplitudes involved are very small. Grain crushing is predominantly produced by the full displacement installation process.

The mobilization of local friction along the interface during the cyclic sequence is mainly the result of the combination of the evolution of two quantities: the progressive decrease, due to cyclic contractancy, of the normal component of the average effective stress,  $\sigma'_n$ , as materialized by the elongation of the spring and the progressive densification of the sand within the interface zone, also resulting from cyclic contractancy. There is, in fact, competition between these two mechanisms, the decrease in  $\sigma'_n$  promoting the degradation of friction or “cyclic softening”, the densification of the soil, on the other side, promoting dilating behavior and “cyclic hardening”, resulting from partially prevented dilatancy.

The initial thickness of the interface zone is equal to  $t_0$  (Fig. 6). In the initial softening phase, the decrease in  $\sigma'_n$ , corresponding to a decrease of interface thickness ( $t < t_0$ ) is predominant, which results in the cyclic softening observed. The shape of the cycles shows however that, during loading phases upon pushing in and pulling out, the controlling mechanism is partially prevented dilation of the sand (concavity of the curves oriented upward). A point is reached, corresponding to the maximum degradation ( $t = t_1$ , Fig. 6), corresponding to a state where the sand is already well densified, and where the decrease of  $\sigma'_n$  slows down (sand densification on each cycle is becoming less and less important). From this point, the sand in the interface zone continues to densify at low rate (corresponding to a low decrease of  $t$ ) and its dilatant character thus keeps increasing, even slightly, from one cycle to another. As the mechanism involved here is partially prevented dilatancy [23,24], this phenomenon becomes predominant with respect to the reduction of  $\sigma'_n$  and causes progressive hardening of the interface with re-increase of the maximum values of mobilized friction until the end of the sequence, for very large numbers of cycles.

## 5. Conclusion

Based on displacement-controlled cyclic loading tests carried out on a pile-probe jacked into large size samples of sand (simulating the installation of full-displacement piles) reconstituted in a calibration chamber, we were able to observe, after an initial phase of degradation of local interface friction (cyclic softening), and for large numbers of cycles applied, a phenomenon, not yet described, of friction reinforcement corresponding to a cyclic hardening of the interface. This feature, observed on the typical tests presented, is representative of the predominant behaviors observed on a whole set of data corresponding to a complete experimental program, carried out within the SOLCYP research project. The maximum local friction mobilized passes through a minimum and then increases again, continuously, up to very large numbers of cycles ( $10^5$  cycles). This result, as applied to piles, would have important consequences concerning the behaviour of piles submitted to large numbers of cycles. In particular, there would not be a continuous degradation of friction during the cyclic loading, as usually admitted, but, instead, a subsequent reinforcement phase following the degradation, which is rather on the security side. This result has been interpreted in terms of partially prevented dilatancy, based on a conceptual model taking into account an interface zone constrained by a constant rigidity-controlled normal effective stress and the competition existing between two phenomena which are the reduction in normal stress due to cyclic contractancy of the sand and the progressive densification of the latter, which increases its dilatant behaviour. In the initial phase of degradation (cyclic softening), the influence of normal stress reduction would be predominant and in the phase of cyclic hardening, the partially prevented dilatant behavior would be predominant. Even if, quantitatively, observations that would be done on a real size pile could be different from those made on the pile-probe (different rigidity for the real size pile and the pile-probe), the same qualitative trends should however be observed, which could be the object of further experimental research.

## Acknowledgements

The present work was undertaken within the framework of the French ANR research project SOLCYP whose support is greatly acknowledged by the authors.



## References

- [1] S.F. Chan, T.H. Hanna, Repeated loading on single piles in sand, *J. Geot. Eng. Div., ASCE* 106 (2) (1980) 171–188.
- [2] J.F. Nauroy, F. Brucy, P. Le Tirant, Static and cyclic load tests on a drilled and grouted pile in calcareous sand, in: *Proc. of the 4th Int. Conf. on the Behaviour of Offshore Structures*, 1985, pp. 577–587.
- [3] K. Karlsrud, F. Nadim, T. Haugen, Piles in clay under cyclic axial loading – Field tests and computational modelling, Norwegian Geotechnical Institute, 1987, Publication n° 169.
- [4] K.H. Andersen, A. Kleven, D. Heien, Cyclic soil data for design of gravity structures, *J. Geot. Eng. Div., ASCE* 114 (5) (1988) 517–539.
- [5] R.G. Bea, Pile capacity for axial cyclic loading, *J. Geot. Eng. Div., ASCE* 118 (1) (1992) 34–50.
- [6] F.M. Randolph, H.A. Joer, M.S. Khorshid, A.M. Hyden, Field and laboratory data from pile load tests in calcareous soil, in: *Proc. 28th Offshore Technology Conference*, Texas, USA, 1996, pp. 327–336.
- [7] J.T. Chin, H.G. Poulos, Tests on model jacked piles in calcareous sand, *Geot. Testing J.* 19 (2) (1996) 164–180.
- [8] M. Uesugi, H. Kishida, Y. Tsubakihara, Friction between sand and steel under repeated loading, *Soils Found.* 29 (3) (1989) 127–137.
- [9] K. Fakharian, E. Evgin, Cyclic simple-shear behavior of sand–steel interfaces under constant normal stiffness condition, *J. Geot. Geoenviron. Eng., ASCE* 123 (12) (1997) 1096–1105.
- [10] G. Mortara, A. Mangiola, V.N. Ghionna, Cyclic shear stress degradation and post-cyclic behaviour from sand–steel interface direct shear tests, *Can. Geot. J.* 44 (7) (2007) 739–752.
- [11] R.H. Al-Douri, H.G. Poulos, Predicted and observed cyclic performance of piles in calcareous sand, *J. Geot. Eng. Div., ASCE* 121 (1) (1995) 1–16.
- [12] A. Le Kouby, J. Canou, J.-C. Dupla, Behaviour of model piles subjected to cyclic loading, in: *Proc. Int. Conf. on Cyclic Behaviour of Soils and Liquefaction Phenomena*, Bochum, Germany, 2004, pp. 159–166.
- [13] B.M. Lehane, D.J. White, Lateral stress changes and shaft friction for model displacement piles in sand, *Can. Geot. J.* 42 (2005) 1039–1052.
- [14] P.Y. Foray, C.H.C. Tsuha, M. Silva, R.J. Jardine, Z.X. Yang, Stress paths measured around a cyclically loaded pile in a calibration chamber, in: *Physical Modelling in Geotechnics*, London, 2010, pp. 933–939.
- [15] H.W. Koreck, P. Schwartz, Axial cyclic loaded piles, in: *Proc. Int. Conf. on Deep Foundations on Bored and Augered Piles*, 1988, pp. 395–399.
- [16] R. Jardine, J.R. Standing, Pile load performed for HSE cyclic loading study at Dunkirk (France), *Offshore Technology Report*, vol. 2, 2000.
- [17] C.Y. Lee, H.G. Poulos, Experimental investigations of axial capacity of model grouted piles in marine calcareous sediments, *Research report R618*, University of Sydney, 1990.
- [18] J.C. Dupla, J. Canou, Cyclic pressuremeter loading and liquefaction properties of sands, *Soils and Foundations* 43 (2) (2003) 17–31.
- [19] T. Le Thiet, J. Canou, J.-C. Dupla, Study of pile vibrodriving process in a calibration chamber, in: *Proc. 16th Int. Conf. on Soil Mechanics and Geotech. Eng.*, Osaka, 2005, pp. 823–826.
- [20] B. Tali, Comportement de l'interface sol–structure sous sollicitations cycliques. Application au calcul des fondations profondes, Ph.D. thesis, Université Paris-Est, Ecole des Ponts ParisTech, 2011.
- [21] B.M. Lehane, R.J. Jardine, A.J. Bond, R. Frank, Mechanisms of shaft friction in sand from instrumented pile tests, *J. Geot. Eng. Div., ASCE* 119 (1) (1993) 19–35.
- [22] D.J. White, B.M. Lehane, Friction fatigue on displacement piles in sand, *Géotechnique* 54 (10) (2004) 645–658.
- [23] M. Boulon, P. Foray, Physical and numerical simulation of lateral shaft friction along offshore pile in sand, in: *Proc. 3rd Int. Conf. on Numerical Methods in Offshore Piling*, Nantes, France, 1986, pp. 127–147.
- [24] F. Schlosser, A. Guilloux, Le frottement dans le renforcement des sols, *Rev. Fr. Géotech.* 16 (1980) 65–77.